

Symmetry Analysis of the Kohn-Sham Band Structure of Bulk Lithium Fluoride

Richard J. Mathar*

Goethestr. 22, 69151 Neckargemünd, Germany

(Dated: November 11, 2018)

Kohn-Sham orbitals of face-centered cubic lithium fluoride are calculated in prototypical local-density approximations to the exchange-correlation functional. The symmetry analysis of these Bloch functions in a LCAO basis on a path Γ -X-W-K- Γ -L-W through the Brillouin Zone is compiled into a list of errata to symmetry labels in the LiF literature, the bulk of which dates back to the 1970's.

PACS numbers: 61.50.Ah, 71.20.Ps, 71.15.Mb

I. SCOPE

The crystallographic symmetry of the ground state of solid lithium fluoride (LiF) is simple: a face-centered cubic Bravais lattice with one formula unit in the primitive unit cell, known as the rock salt structure, space group $Fm\bar{3}m$ and number 225 in the International Tables [1]. Yet the symmetry assignments to the lines and points of symmetry of (effective) single-particle orbitals (wave-functions) populating the reciprocal unit cell vary in the literature to a high degree, with no discussion that would unify the diverging opinions. This work is to be considered an extended erratum to consolidate the graphs of band structures of LiF published in the past that are incoherent or violate rules of the compatibility tables.

We start from self-consistent Kohn-Sham (KS) orbitals obtained in a Local Density Approximation (LDA) to the exchange-correlation (XC) functional of the Density Functional Theory (DFT), and apply the space group operators to points of low and high symmetry in the Brillouin Zone (BZ), which lead to symmetry labels read from the character tables of their little groups. Band structure line graphs result as we connect the Kohn-Sham eigenvalues in accordance with the compatibility tables.

II. KOHN-SHAM ORBITALS IN THE LDA

A. GTOFF Bloch Functions

The basis of this work are the LiF eigenvectors (Bloch functions) and eigenvalues (energies) calculated by the non-relativistic version of GTOFF [2, 3, 4], which solves the self-consistent Kohn-Sham equations with an all-electron LCAO ansatz for the Bloch functions, and builds the atomic orbitals from linear combinations of (Hermite) Gaussian Type primitives. We use its “bulk” option (translational periodicity of the Kohn-Sham Hamiltonian in three directions) and two variants of the LDA, one in the next section merely to demonstrate compatibility of

the outcome with other, independent calculations, and an older one in the main section to make close contact to the Zunger–Freemann publication [5], which, by the number of citations received, could be called the “reference.”

Unless noted otherwise, the results are calculated using a Kohn-Sham basis with 23 Gaussian Type Orbitals GTO's at the Li and 46 GTO's at the F sites (Table I).

B. LDA band gap

The direct band gap E_g at Γ in the Hedin-Lundqvist-type Local Density Approximation (LDA) to the exchange-correlation [6] is found to be

$$E_g/\text{eV} \approx 8.99 - 3.41\Delta + 1.24\Delta^2 \quad (\Delta \equiv a/a_0 - 7.5939)$$

as a function of the lattice parameter $7.37a_0 < a < 8.05a_0$, where a is the edge length of the underlying simple cubic unit cell, where $a/2$ is the shortest distance between Li and F, and a_0 the Bohr radius. (The theoretical equilibrium lattice constant is smaller than $7.37a_0$, hence underestimates the experimental value, $7.60841a_0$ at 25°C [7], by at least 3%. In a recent pseudopotential calculation [8], the deviation is 2.7%.) The value is compatible with the 8.7 eV of a pseudo-potential calculation with the Ceperley-Alder LDA to the exchange-correlation [9] at $a = 7.62a_0$, and values of 8.89 eV (8.82 eV) by an independent Full-Potential Linearized Augmented Plane-Wave program at $a = 7.59a_0$ ($7.61a_0$) for the same energy functional [10].

The band gap of the X_α ($\alpha = 2/3$) calculation is about 1.0 eV smaller than calculated by Zunger and Freeman [5], which probably indicates that their method of calculation starts from parameters of isolated ions and does not achieve full self-consistency at the end. (Their program likewise seemed to over-estimate the direct band gap of cubic boron nitride [11] by ≈ 2 eV compared with the consolidated theoretical result [12, 13, 14, 15] of 8.8 eV, and of diamond [16] by ≈ 0.7 eV compared with other theoretical results [17, 18, 19, 20].)

A considerably smaller theoretical LiF band gap of 7.65 eV has been reported by Ching *et al.* [21] for $a = 7.591a_0$. Assessment of this number is not clear; the optical band gap of MgO is given as 5.13 eV [21], whereas an earlier

*Electronic address: mathar@mpia.de;
URL: <http://www.mpia.de/MIDI/People/mathar>

value by what looks like the same methodology is 4.19 eV [22].

III. SYMMETRY ANALYSIS

A. Character tabulation

Point group labels are determined following [23], including the Errata by Stokes and Hatch [24]. (In addition, σ_z ought be added for X in the Γ_c^f lattice in [23, Tab. 3.6]. Evarestov and Smirnov interchange B_1 and B_2 for C_{6v} in [25, Tab. 3.6] relative to [23, Tab. 2.2]. This is not simply a typo but persists if we compare the C_{6v} entry in [25, Tab. 4.2] with the D_{6h} table of Flurry [26, App. 4]. This does not cause confusion here, as C_{6v} does not enter the subsequent analysis of a cubic space group.)

The computational procedure is to construct the character tables of the ten abstract groups of the lines/points of symmetry in the Brillouin Zone according to [23, p. 389]. An eleventh entry of the form

$$O \quad \mathbf{G}_2^1 : (\sigma_z, 0) \dots : c$$

is added to account for points in the O -plane [23, Tab. 3.11] that we meet walking from W to K . GTOFF orbitals are rotated to ensure their \mathbf{k} -points fall into the “irreducible” wedge of the BZ defined in [23, Fig. 3.14]. For each class of the abstract group of the \mathbf{k} -point, a character of the GTOFF orbital (Bloch function) $\langle \mathbf{r} | \nu \mathbf{k} \rangle$ of band ν is computed as the integral $\sum_d \langle \nu \mathbf{k} | \{R|\mathbf{v}\} | \nu \mathbf{k} \rangle$, applying one (any) Seitz operator $\{R|\mathbf{v}\}$ of this class. The sum d over up to three degenerate levels deals automatically with some arbitrariness of the pointing directions of the eigenstates/eigenvectors in these cases that has been left over from use of a (generic) eigenvalue routine in the GTOFF solver. Since GTOFF employs (Hermite) Cartesian Gaussians in the molecular basis, the point operators R are adequately represented by Cartesian, matrices: Operation of these on the bases is a multinomial re-expansion in the x , y , and z coordinates [23, Sec. 1.4]. All operators R are members of the little co-group; therefore $\{R|\mathbf{v}\} | \nu \mathbf{k} \rangle$ is another Bloch function at the same \mathbf{k} , and the integrals (matrix elements) become standard LCAO overlap integrals.

This determination of characters associated with a list of Seitz operators is numerically stable. Matrix representations of the abstract groups are not needed. It does not work blindly in cases of [23, Tab. 5.7] where the authors chose generators of the abstract group that are not space group operators: consider the example of Q^x of space group 227: the translation $\mathbf{v} = (\frac{1}{4}, \frac{1}{4}, \frac{1}{4})$ has been removed from $R = C_{2f}$, and the overlap integral cannot “recover” the missing overall phase factor associated with this virtual relocation of the rotated image. (In fact, all pair-wise overlap integrals become wrong caused by incorrect distances between the Wyckoff positions in the “bra” and the “ket.”) The alternative is comparison

of the Bloch function and its rotated image in selected regions of the BZ, but this calls for more advanced methods of “important sampling” to bypass nodes of the orbitals or dispose regions of small orbital density (in case of strongly localized core orbitals).

The representation of the abstract group that matches this list of characters is translated to a point group symbol by [23, Tab. 5.8]. Subduction frequencies (compatibility tables) are generated from the point group genealogy [23, Fig. 4.1] and [27, (4.3)] for adjacent points on the BZ path.

B. Symmetry assignments and level crossing

The band structure of Fig. 1 ensues in compliance with the compatibility tables [26, 27, 28, 29, 30]. Lines are the linear (tetrahedral) interpolations/connections obtained from the symmetry analysis; so there is no finesse in regions where perturbation theory proves that there is no linear term in the series expansion of the energy as a function of \mathbf{k} . Point groups labels follow [23] and may be converted to the convention of Bouckaert *et al.* [29] using Tab. II. The symmetry labels refer to a setting with a Li atom at the origin of coordinates, and are not always unique. The state near -11 eV at L , for example, consists of p -orbitals on the F site plus some s -contribution on the Li site. This Bloch-type KS orbital is even under inversion at *this* origin. If a F atom is chosen to define the origin of coordinates, this same KS orbital is odd under inversion at this new origin, and labels have to be swapped as follows [25, Tab. 4.7][31][32, Fig. 5]: $A_1 \leftrightarrow B_2$, $A_2 \leftrightarrow B_1$ (at W); $A_{2u} \leftrightarrow A_{1g}$, $E_g \leftrightarrow E_u$ (at L); $A \leftrightarrow B$ (at Q).

The solid lines in Fig. 1 are derived following a non-crossing rule for energy dispersions of the same symmetry [33]. The rule applies perturbation theory to deduce that in almost all cases there is some residual interaction build into the Hamiltonian that splits energy levels that close up. This argument of [33, Sec. 1] does not apply to the cases of empty orbitals—the simplest demonstration are the level crossings in empty lattices (Fig. 4.4.3 in [34])—that are eigenstates of the full/complete (self-consistent) 1-particle Hamiltonian. Our ground state Hamiltonian does *not* include any mechanism (term) to lift two electrons to the crossing regions to modify the energetically degenerate orbitals. Dashed lines above 25 eV indicate some (but not all) alternative choices, if “accidental” degeneracies are not ruled out. To decide which of these connections are “correct,” various approaches are helpful. (i) According to $\mathbf{k} \cdot \mathbf{p}$ perturbation theory, the overlap $\langle \nu \mathbf{k} | \nu' \mathbf{k} + \mathbf{q} \rangle$ will be close to 1 in a neighbourhood of small \mathbf{q} around a \mathbf{k} -value, if the correct band $\nu = \nu'$ is chosen. In practice, however, the density of the mesh in the reciprocal lattice hardly is dense enough to have sufficiently small $|\mathbf{q}|$ at hand. (ii) One might compute the eigenvalues at an extra intermediate \mathbf{k} -point close to the expected crossing. (iii) The connectivity of bands does

not change when the lattice is set up at a large lattice constant (with almost horizontal bands and therefore a minimum of accidental crossings), then is “adiabatically” contracted to its actual value. With this idea in mind we calculate the same crystal at a larger lattice constant grown to 110% (Fig. 2). The prospective accidental crossing at Q near 28 eV in Fig. 1 is not supported by Fig. 2, because the state A_{2u} at L is still connected to B_2 at W near 23 eV in Fig. 2. (This result is confirmed by the first approach, the inspection and comparison of the dominant basis function of the four states.) In contrast, the two accidental crossings near 32 eV at Λ in Fig. 1 seem actually to exist, as a band of A_1 symmetry with very strong dispersion rapidly moves upwards as a increases, with its local minimum already above 35 eV in Fig. 2. The remaining case nearby 33 eV at Δ in Fig. 1 is not elucidated by Fig. 2; one must increase the lattice constant to about 150% to see that the point with E_u symmetry at X then falls below the point with E_g symmetry and gets connected with T_{2g} at Γ , to indicate that there also is accidental crossing of the two lines with E symmetry nearby 34 eV on the Δ line in Fig. 1.

An additional band of Γ'_2 (A_{2u}) symmetry appears in calculations with a mixed basis set [35] and an Augmented Plane Wave basis ([36], Fig. 1 at 1.9 ryd) which is absent in our Figs. 1 and 2. If we augment our LCAO orbital basis by a full set of five f -orbitals with exponent $2.98632 \cdot 10^{-1}$ at the F sites, it also emerges from our calculations, 18.6 eV above the $\Gamma_{1,c}$ bottom of the conduction band. This basis set completion problem affects calculations of dielectric matrices that sum over unoccupied states [37].

The choice of an X_α -type LDA in Fig. 1 and 2 is not to promote simplistic density functions, but for immediate comparison with the graph in [5] and since this could serve as a common standard reference of DFT implementations.

C. Discussion

A tour through the literature in roughly chronological order—strictly confined to work that lists eigenvalues or band structures—leads to the following comparison:

- [32] Fig. 5 is compatible with our results.
- [36] The L-labels in Fig. 1 suggest Page and Hygh use a setting with Li in the center of coordinates: W_1 near -0.45 ryd should read W'_2 .
- [38] The results in Tab. 1 and Fig. 3 are compatible with ours. Chaney *et al.* did not include d -type basis functions, which means the T_{2g} point near 15 eV in our Fig. 1 and bands that are attached to it disappear. In consequence they neither show a Γ'_{25c} nor a X_{3c} in Tab. 1. Our Fig. 3 illustrates this case. The d -orbitals are obviously a key ingredient

to construct an even function at Γ in the conduction band, with otherwise only s -hybrids remaining which have to stay orthogonal to the three s -type core orbitals.

- [39] Figs. 1, 3 and 6: the upper L'_2 should read L_1 . (The compatibility relations would allow the connection $\Gamma_1-\Lambda_1-L'_2$.) The equivalent correction in Tab. VIII is to exchange $L'_3 \rightarrow L'_2$ with $L'_3 \rightarrow L_1$ in the first column.
- [40, 41] The results in Tab. 1 are compatible with those here in the same sense as discussed for [38].
- [42] Figs. 1 and 2: the upper L'_2 should read L_1 . Tab. 1: replace L'_{2c} by L_{1c} .
- [43] Figs. 3 and 4 are compatible with our analysis.
- [44] Fig. 1: the 1 at X should read $4'$. A comment on the 3 at X and L is difficult because the order of their Hartree-Fock energy levels might be switched in comparison to our DFT results.
- [45] The label X_3 in Tab. IV should read X'_4 where they refer to their own results, as their basis does not include d -orbitals, see the discussion of [38].
- [46] Figs. 2 and 3: the uppermost X'_4 should read X_1 . (The compatibility relations would allow the connection $\Gamma_{15}-\Delta_1-X'_4$.) The uppermost L'_3 should read L_3 . The middle L'_2 near 10 eV should read L_1 .
- [47] In the LiF part of Fig. 2, the 1 at X should read $4'$. (The compatibility relations would allow the connection $\Gamma_1-\Delta_1-X_1$.)
- [48] This tight-binding analysis of the valence bands confirms our results.
- [49] The lower L'_3 in Fig. 8 should be replaced by L'_2 , and the X_1 by X'_4 .
- [5] The labels at L should read (bottom-up) $L_1, L'_2, L'_3, L_1, L'_2, L_3, L'_2$, and L'_3 in Fig. 2. All three cases of L_3 and L'_3 should split towards Q. There should be no crossing at Q near 7 eV. The Δ -lines near 12 eV should twist to connect X_3 to Γ'_{25} by Δ'_2 and X_1 to Γ_{15} by Δ_1 . The labels Σ_2 and Σ_3 near 17 eV should probably be exchanged. In Tab. 1, all X_4, X_5 and L_2 , also L_{3v} should be primed. $X_{1,c}$ in Tab. 1 should read $X_{3,c}$ where it refers to their own calculations, which follows from measuring the vertical distance in Fig. 2 and comparison with the value of 0.710 hartree given in the table. (See again the comment on [38].)
- [31] Fig. 3 is compatible with our labeling scheme.
- [50] In Fig. 2, the upper L'_2 should read L_1 .
- [51] Fig. 1 is reproduced from [5]; hence the same comments hold.

- [8] The following LDA lines in Fig. 1 should cross: Z lines near 41 eV; O lines near 41 eV; Σ lines near 30 eV and 39 eV; Σ lines close to K near 35 eV.

Acknowledgments

We thank Peter Blaha for providing us with results of his independent calculation. Jonathan Boettger's main-

tenance of the GTOFF code was an indispensable foundation of the present analysis.

-
- [1] T. Hahn, ed., *International Tables for Crystallography*, vol. A (Kluwer Academic Publishers, Dordrecht, The Netherlands, 2002).
- [2] J. C. Boettger, Phys. Rev. B **53**, 3007 (1996).
- [3] J. C. Boettger, Int. J. Quant. Chem. **60**, 1345 (1996).
- [4] J. C. Boettger, Int. J. Quant. Chem. Symp. **29**, 197 (1995).
- [5] A. Zunger and A. J. Freeman, Phys. Rev. B **16**, 2901 (1977).
- [6] V. L. Moruzzi, J. F. Janak, and A. R. Williams, *Calculated Electronic Properties of Metals* (Pergamon, New York, 1978).
- [7] W. Pies and A. Weiss (Springer, Berlin, 1973), vol. III/7a of *Zahlenwerte und Funktionen aus Naturwissenschaften und Technik, Neue Serie*, chap. 1.1, p. 1.
- [8] N.-P. Wang, M. Rohlfing, P. Krüger, and J. Pollmann, Phys. Rev. B **67**, 115111 (2003).
- [9] E. L. Shirley, L. J. Terminello, J. E. Klepeis, and F. J. Himpsel, Phys. Rev. B **53**, 10296 (1996).
- [10] P. Blaha (1998), priv. commun.
- [11] A. Zunger and A. J. Freeman, Phys. Rev. B **17**, 2030 (1978).
- [12] K. Kim, W. R. L. Lambrecht, and B. Segall, Phys. Rev. B **53**, 16310 (1996).
- [13] P. Rodríguez-Hernández, M. González-Díaz, and A. Muñoz, Phys. Rev. B **51**, 14705 (1995).
- [14] J. Furthmüller, J. Hafner, and G. Kresse, Phys. Rev. B **50**, 15606 (1995).
- [15] K. T. Park, K. Terakura, and N. Hamada, J. Phys. C **20**, 1241 (1987).
- [16] A. Zunger and A. J. Freeman, Phys. Rev. B **15**, 5049 (1977).
- [17] M. R. Salehpour and S. Satpathy, Phys. Rev. B **41**, 3048 (1990).
- [18] M. P. Surh, S. G. Louie, and M. L. Cohen, Phys. Rev. B **43**, 9126 (1991).
- [19] M. Willatzen, M. Cardona, and N. E. Christensen, Phys. Rev. B **50**, 18054 (1994).
- [20] R. J. Mathar, arXiv:cond-mat/0007153 (2000).
- [21] W. Y. Ching, F. Gan, and M.-Z. Huang, Phys. Rev. B **52**, 1596 (1995).
- [22] Y.-N. Xu and W. Y. Ching, Phys. Rev. B **43**, 4461 (1991).
- [23] C. J. Bradley and A. P. Cracknell, *The Mathematical Theory of the Symmetry in Solids* (Clarendon Press, Oxford, 1972).
- [24] H. T. Stokes and D. M. Hatch, *Isotropy Subgroups of the 230 Crystallographic Space Groups* (World Scientific, Singapore, 1988).
- [25] R. A. Evarestov and V. P. Smirnov, *Site Symmetry in Crystals*, vol. 108 of *Springer Series in Solid State Sci-*
ences (Springer, Berlin, Heidelberg, 1993).
- [26] R. L. Flurry, *Symmetry Groups* (Prentice Hall, Englewood Cliffs, NJ, 1980).
- [27] G. F. Koster, J. O. Dimmock, R. G. Wheeler, and H. Statz, *Properties of the thirty-two point groups* (MIT Press, Cambridge, 1963).
- [28] A. P. Cracknell, *Group Theory in Solid-State Physics* (Taylor & Francis, London, 1975).
- [29] L. P. Bouckaert, R. Smoluchowski, and E. Wigner, Phys. Rev. **50**, 58 (1936).
- [30] J. A. Salthouse and M. J. Ware, *Point Group Character Tables* (Cambridge University Press, Cambridge, 1972).
- [31] S. Antoci and L. Mihich, Phys. Rev. B **21**, 799 (1980).
- [32] D. H. Ewing and F. Seitz, Phys. Rev. **50**, 760 (1936).
- [33] C. Herring, Phys. Rev. **52**, 365 (1937).
- [34] J. Callaway, *Quantum Theory of the Solid State* (Academic Press, New York, San Francisco, 1976).
- [35] A. B. Kunz, T. Miyakawa, and S. Oyama, Phys. Stat. Sol. **34**, 581 (1969).
- [36] L. J. Page and E. H. Hygh, Phys. Rev. B **1**, 3472 (1970).
- [37] L. Reining, G. Onida, and R. W. Godby, Phys. Rev. B **56**, R4301 (1997).
- [38] R. C. Chaney, E. E. Lafon, and C. C. Lin, Phys. Rev. B **4**, 2734 (1971).
- [39] D. M. Drost and J. L. Fry, Phys. Rev. B **5**, 684 (1972).
- [40] W. P. Menzel, C. C. Lin, D. F. Fouquet, E. E. Lafon, and R. C. Chaney, Phys. Rev. Lett. **30**, 1313 (1973).
- [41] W. P. Menzel, C. C. Lin, D. F. Fouquet, E. E. Lafon, and R. C. Chanel, Phys. Rev. Lett. **31**, 340 (1973).
- [42] N. E. Brener, Phys. Rev. B **7**, 1721 (1973).
- [43] G. E. Laramore and A. C. Switendick, Phys. Rev. B **7**, 3615 (1973).
- [44] D. J. Mickish, A. B. Kunz, and T. C. Collins, Phys. Rev. B **9**, 4461 (1974).
- [45] R. N. Euwema, G. G. Wepfer, G. T. Surratt, and D. L. Wilhite, Phys. Rev. B **9**, 5249 (1974).
- [46] N. E. Brener, Phys. Rev. B **11**, 1600 (1975).
- [47] A. B. Kunz, Phys. Rev. B **12**, 5890 (1975).
- [48] S. T. Pantelides, Phys. Rev. B **11**, 5082 (1975).
- [49] M. Piacentini, D. W. Lynch, and C. G. Olson, Phys. Rev. B **13**, 5530 (1976).
- [50] A. B. Kunz, Phys. Rev. B **26**, 2056 (1982).
- [51] J. J. M. Michiels, L. Hedin, and J. E. Inglesfield, Phys. Rev. B **50**, 11386 (1994).
- [52] H. Partridge, J. Chem. Phys. **90**, 1043 (1989).
- [53] H. Partridge, *NASA Technical Memorandum 1.15:101044*, Ames Research Center, Moffett Field (1989).

type	Li		F	
	exponent	coefficient	exponent	coefficient
s	$7.471871 \cdot 10^4$	0.000006	$4.007457 \cdot 10^5$	0.0000114
	$1.11883 \cdot 10^4$	0.000044	$6.001308 \cdot 10^4$	0.0000904
	$2.546139 \cdot 10^3$	0.000232	$1.36574 \cdot 10^4$	0.0004719
	$7.211808 \cdot 10^2$	0.000978	$3.868237 \cdot 10^3$	0.001991
	$2.352752 \cdot 10^2$	0.003545	$1.261848 \cdot 10^3$	0.0071938
	$8.493513 \cdot 10^1$	0.011395	$4.554532 \cdot 10^2$	0.0229084
	$3.312063 \cdot 10^1$		$1.775331 \cdot 10^2$	
	$1.371652 \cdot 10^1$		$7.345899 \cdot 10^1$	
	$5.941083 \cdot 10^0$		$3.181364 \cdot 10^1$	
	$2.651974 \cdot 10^0$		$1.426084 \cdot 10^1$	
	$1.209217 \cdot 10^0$		$6.478246 \cdot 10^0$	
	$5.56503 \cdot 10^{-1}$		$2.627737 \cdot 10^0$	
	$2.37586 \cdot 10^{-1}$		$1.184078 \cdot 10^0$	
p	$3.337598 \cdot 10^1$		$6.600857 \cdot 10^2$	0.0001863
	$7.907316 \cdot 10^0$		$1.564625 \cdot 10^2$	0.0015866
	$2.50156 \cdot 10^0$		$5.065363 \cdot 10^1$	0.008512
	$8.8178 \cdot 10^{-1}$		$1.908092 \cdot 10^1$	
	$3.30977 \cdot 10^{-1}$		$7.872742 \cdot 10^0$	
			$3.449055 \cdot 10^0$	
			$1.544895 \cdot 10^0$	
			$6.86529 \cdot 10^{-1}$	
			$2.98632 \cdot 10^{-1}$	
			$1.24571 \cdot 10^{-1}$	
d			$2.98632 \cdot 10^{-1}$	
			$1.24571 \cdot 10^{-1}$	

TABLE I: Exponentials and contraction coefficients of GTO's centered at F and Li, derived from Partridge's 13s9p and 15s10p sets [52, 53].

W	L	X	Γ	K(Σ)	Z	Δ	Λ
$\bar{4}2m$	$\bar{3}m$	$4/mmm$	$m\bar{3}m$	$mm2$	$mm2$	$4mm$	$3m$
A ₁ W ₁	A _{1g} L ₁	A _{1g} X ₁	A _{1g} Γ_1	A ₁ K ₁	A ₁ Z ₁	A ₁ Δ_1	A ₁ Λ_1
B ₁ W ₁	A _{2g} L ₂	B _{1g} X ₂	A _{2g} Γ_2	A ₂ K ₂	A ₂ Z ₂	B ₁ Δ_2	A ₂ Λ_2
A ₂ W ₂	E _g L ₃	B _{2g} X ₃	E _g Γ_{12}	B ₂ K ₃	B ₁ Z ₃	B ₂ Δ'_2	E Λ_3
B ₂ W ₂	A _{1u} L ₁	A _{2g} X ₄	T _{1g} Γ'_{15}	B ₁ K ₄	B ₂ Z ₄	A ₂ Δ'_1	
E W ₃	A _{2u} L ₂	A _{1u} X ₁	T _{2g} Γ'_{25}			E Δ_5	
	E _u L ₃	B _{1u} X ₂	A _{1u} Γ'_1				
		B _{2u} X ₃	A _{2u} Γ'_2				
		A _{2u} X ₄	E _u Γ'_{12}				
		E _g X ₅	T _{1u} Γ_{15}				
		E _u X ₅	T _{2u} Γ_{25}				

TABLE II: The interpretation of the point group symbols of [23] in terms of those used in [29], obtained by searching for matching lines in the character tables. There is only one table for $mm2$ in [23, p. 58] and only one common table for Z and K in [29, Tab. VI], but the σ_x and σ_z operations are in different classes in [29, Tab. VI], which leads to two separate columns for Z and K here.

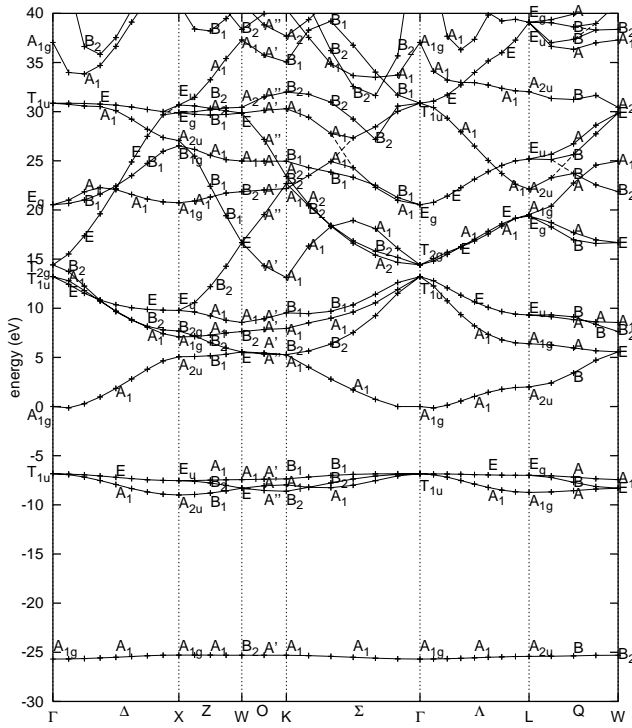


FIG. 2: KS band-structure of LiF as in Fig. 1 for a 10% larger lattice constant. As the lattice constant increases, the bottom of the conduction band at Γ becomes a local maximum with satellite minima at the adjacent Δ , Σ and Λ lines.

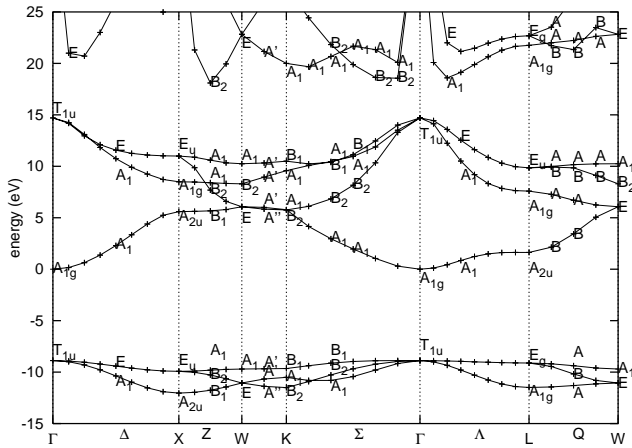


FIG. 3: KS band-structure of LiF as in Fig. 1 but the basis of Tab. I replaced by a smaller basis of Li $11s4p$ (contracted 41111111/1111) and F $13s8p$ (4111111111/2111111) to illustrate the role of F d -orbitals.